JAST (Journal of Animal Science and Technology) TITLE PAGE

Upload this completed form to website with submission

ARTICLE INFORMATION	Fill in information in each box below
Article Type	Research article
Article Title (within 20 words without abbreviations)	A TMAH-Chloroform Sample-Preparation Workflow for Nile Red-Based Screening of Microplastics in Animal Feed
Running Title (within 10 words)	Fluorescence-Based Detection of Microplastics in Animal Feed
Author	Veysel Doğan[1]
Affiliation	[1] Department of Animal Nutrition and Nutritional Diseases, Faculty of Veterinary Medicine, Kastamonu University, Kastamonu, Türkiye
ORCID (for more information, please visit https://orcid.org)	Veysel Doğan (https://orcid.org/0000-0002-1148-5416)
Competing interests	The author declares that there are no competing interests.
Funding sources State funding sources (grants, funding sources, equipment, and supplies). Include name and number of grant if available.	The research received no external funding.
Acknowledgements	The author gratefully acknowledges Prof. Dr. Meral Yurtsever for providing access to laboratory facilities and her valuable comments on the manuscript.
Availability of data and material	Upon reasonable request, the datasets of this study can be available from the corresponding author.
Authors' contributions Please specify the authors' role using this form.	Conceptualization: Doğan V. Data curation: Doğan V. Formal analysis: Doğan V. Methodology: Doğan V. Software: Doğan V. Validation: Doğan V. Investigation: Doğan V. Writing - original draft: Doğan V. Writing - review & editing: Doğan V.
Ethics approval and consent to participate	This study did not involve human participants or live animals. Therefore, ethics committee approval was not required.
Declaration of generative AI	During the preparation of this work, ChatGPT was used for language editing and improving readability. The author reviewed and edited the content as needed and takes full responsibility for the content of the publication.

ACCEPTED

CORRESPONDING AUTHOR CONTACT INFORMATION

For the corresponding author (responsible for correspondence, proofreading, and reprints)	Fill in information in each box below
First name, middle initial, last name	Veysel Doğan
Email address – this is where your proofs will be sent	d_veysel@yahoo.com
Secondary Email address	vdogan@kastamonu.edu.tr
Address	Department of Animal Nutrition and Nutritional Diseases, Faculty of Veterinary Medicine, Kastamonu University, Kastamonu, Türkiye

Cell phone number	0090 533 060 2480
Office phone number	0090 366 280 6029
Fax number	

ACCEPTED

Abstract

Animal feed is increasingly recognized as an important route of microplastic (MP) exposure in livestock production systems; however, reliable fluorescence-based detection remains challenging because proteins, lipids, pigments, and other organic constituents interfere with fluorescence analyses. This study developed and evaluated a sample-preparation protocol combining tetramethylammonium hydroxide (TMAH) digestion with chloroform (TCM) extraction to reduce matrix interference while preserving the fluorescence characteristics of MP particles prior to Nile Red (NR) staining. The protocol was evaluated using five commercially available animal feeds (layer, broiler, calf starter, calf grower, and turkey feeds) and four representative polymers: polyethylene (PE), polypropylene (PP), polystyrene (PS), and polyethylene terephthalate (PET). Fluorescence microscopy, quantitative fluorescence intensity measurement, linear regression analysis, and discriminant function analysis were used to assess the analytical performance of the proposed workflow. The evaluated protocol reduced matrix-derived fluorescence interference and enabled clear visualization of NR-positive particles without significantly altering the fluorescence responses of the reference polymers. Among the tested polymers, PS exhibited the highest fluorescence intensity (174.69 ± 20.91), followed by PP (143.21 ± 37.74), PE (134.03 ± 38.36), and PET (117.59 ± 36.93). Significant differences in fluorescence intensity were observed among polymer types ($p < 0.05$), and discriminant function analysis demonstrated that fluorescence intensity can serve as a complementary analytical parameter for polymer differentiation, although classification accuracy remained moderate (47%). Collectively, the proposed TMAH-TCM workflow provides a practical sample-preparation approach for NR-based screening of MP in animal feed matrices, while fluorescence intensity may provide complementary information for preliminary polymer differentiation.

Keywords: Microplastic, Animal Feeds, Fluorescence Microscopy, Nile Red, One Health, Nutrition

ACCEPTED

Introduction

Microplastics (MPs) have emerged as ubiquitous environmental contaminants and have been detected in both aquatic and terrestrial ecosystems (1,2). Increasing evidence indicates that terrestrial exposure is becoming equally important, particularly in agricultural systems where plastics are extensively used for silage production, mulching, irrigation, feed storage, and other farming practices (3). Consequently, livestock are continuously exposed to MPs through contaminated feed, water, and the surrounding farm environment (4). Recent studies have confirmed the presence of polymer particles in common feed materials, including corn silage, hay, and protein-rich feedstuffs (5), while experimental studies have demonstrated that MPs can be transferred from contaminated soils into plants, creating an

additional pathway for feed contamination (6). These findings identify animal feed as an important, yet still insufficiently investigated, route of MP exposure in livestock production systems.

Growing evidence indicates that ingested MPs may adversely affect animal health following chronic exposure. Experimental evidence has demonstrated gastrointestinal injury, intestinal inflammation, oxidative stress, metabolic disturbances, reproductive impairment, and tissue accumulation in several organs following MP exposure (4,7–10). In lambs, PS exposure has been associated with gastrointestinal damage, reduced daily weight gain, altered blood parameters, impaired meat quality, and intestinal microbial imbalance (11). Beyond animal health, the accumulation of MPs in livestock raises concerns regarding their transfer into foods of animal origin and the subsequent implications for human health (12). Therefore, reliable monitoring of MP contamination in animal feed has become increasingly important for safeguarding both animal production and food safety.

Accurate identification of MPs in feed materials remains analytically challenging because animal feeds contain a complex mixture of proteins, lipids, pigments, carbohydrates, and other organic constituents that interfere with sample preparation and analytical detection. Currently, several analytical techniques, including Fourier-transform infrared spectroscopy (FTIR), Raman spectroscopy, pyrolysis-gas chromatography-mass spectrometry (Py-GC/MS), and fluorescence microscopy, are widely employed for MP identification (13–16). Among these techniques, fluorescence microscopy using NR has become one of the most widely adopted approaches because it is rapid, inexpensive, and suitable for screening large numbers of samples (17,18). However, because NR is a lipophilic dye, it readily binds not only to plastic particles but also to lipids and other hydrophobic organic compounds, thereby increasing the risk of false-positive fluorescence in complex biological matrices (19–21). Consequently, efficient removal of matrix-derived organic matter before NR staining is essential for improving the specificity of fluorescence-based MP screening.

Despite the increasing application of NR fluorescence microscopy for MP detection, reliable analysis of animal feed remains limited by the absence of standardized sample-preparation workflows capable of efficiently removing matrix-derived organic interference while preserving polymer fluorescence responses. Existing extraction methods have primarily been developed for water, sediment, and soil samples and frequently require further optimization before they can be successfully applied to feed matrices because of substantial differences in their chemical composition (22,23). Variations in protein, lipid, fiber, and pigment contents may markedly influence extraction efficiency, staining specificity, and fluorescence response. Consequently, developing a sample-preparation workflow capable of efficiently removing matrix-derived organic interference while preserving the fluorescence response of MPs remains a critical analytical challenge.

ACCEPTED

Accordingly, the present study aimed to develop and evaluate a sample-preparation workflow combining TMAH digestion with TCM extraction for NR-based detection of MP particles in animal feed. The proposed workflow was evaluated using five commercially available animal feeds and four representative polymers (PE, PP, PS, and PET) prepared from commercially available plastic products. In addition, fluorescence intensity was quantitatively assessed to determine whether it could serve as a complementary analytical parameter for polymer differentiation following extraction. We hypothesized that the proposed TMAH-TCM workflow would reduce matrix-derived organic interference while preserving the fluorescence response of reference polymer particles, thereby facilitating fluorescence-based screening and preliminary differentiation among polymer types. The findings of this study provide a practical sample-preparation approach for NR-based screening of MPs in complex animal feed matrices while demonstrating the potential of fluorescence intensity as a complementary parameter for preliminary polymer differentiation.

ACCEPTED

Materials and Methods

Feed Samples

Five commercially available concentrate feeds representing different livestock species (layer, broiler, calf starter, calf grower, and turkey feeds) were purchased from local feed suppliers (**Table 1**). Upon arrival at the laboratory, all feed samples were dried at 60 °C overnight, ground using a laboratory mill, and sieved through a 125-µm stainless-steel sieve. The resulting fine fractions were collected and stored in pre-cleaned borosilicate glass tubes until analysis.

To evaluate the analytical performance of the proposed workflow under different matrix conditions, four experimental sample types were prepared for each polymer (i) individual polymer particles (PE, PP, PS, and PET), (ii) a mixed-polymer preparation (PolyMix) containing PE, PP, PS, and PET, (iii) feed samples artificially fortified with the PolyMix preparation (Fortified feed), and (iv) non-fortified commercial feed samples (Feed). This experimental design enabled comparison of fluorescence responses before and after extraction and assessment of the influence of the feed matrix on polymer detection.

For preparation of the fortified samples, 50.0 g of one representative feed was spiked with 0.4 mg of PolyMix consisting of 0.1 mg each of PE, PP, PS, and PET. The fortified feed was homogenized by intermittent shaking over 12 h to ensure uniform distribution of polymer particles prior to extraction. The 0.4 mg fortification level was selected for analytical purposes rather than to simulate environmental exposure and provided equal representation of the four reference polymers (0.1 mg each) within the fortified feed matrix.

Preparation of Reference Polymer Particles

Four commonly encountered polymers (PE, PP, PS, and PET) were selected as representative reference polymers for method development (24). Commercially available single-use plastic products representative of each polymer type was thoroughly rinsed with filtered ultrapure water, cryogenically frozen in liquid nitrogen, and ground into fine particles using a laboratory mill (Sinbo SCM-2934, Türkiye). The resulting particles were sieved using a vibratory sieve, and fractions smaller than 125 µm were collected and stored in pre-cleaned glass bottles until analysis. The particle size ranges of the prepared reference polymer particles are presented in **Table 2**. Particle size was measured from microscopic images using ImageJ and expressed as the maximum particle length (µm).

For fluorescence analyses, three experimental particle preparations were generated: (i) individual reference polymer particles, (ii) PolyMix consisting of equal masses of PE, PP, PS, and PET, and (iii) polymer particles recovered from fortified feed samples following extraction. For the PolyMix preparation, 0.1 mg of each polymer particle type was combined to obtain a total mass of 0.4 mg. Individual polymer particles and PolyMix were dispersed separately in filtered ultrapure water under gentle stirring and subsequently filtered using a vacuum filtration system inside a laminar flow cabinet. To prevent particle loss and cross-contamination, all glassware was sequentially rinsed with filtered ultrapure water, ethanol, acetone, and filtered ultrapure water after each filtration step. All experiments were performed in triplicate.

Reagents

All chemicals were of analytical grade. Ultrapure water was produced using Basic M Up water purification system (MP Minipure, Türkiye) and filtered through membrane filters (Filter-Lab MFV3-047) prior to use. Tetramethylammonium hydroxide (TMAH; 25 wt.% in methanol; Cas No. 75-59-2) and absolute ethanol (Cas No. 64-17-5) were purchased from Merck (Darmstadt, Germany). Acetone (Cas No. 67-64-1) and chloroform (Cas No. 67-66-3) were obtained from Isolab (Eschau, Germany). All reagents were filtered before use and stored in pre-cleaned glass containers to minimize background MP contamination.

Contamination Prevention

Strict quality assurance and contamination control procedures were implemented throughout sampling, sample preparation, and analysis to minimize airborne and laboratory-derived MP contamination. Feed samples were collected and transported in cotton bags to avoid contact with plastic packaging materials. All extraction and filtration procedures were performed inside a laminar flow cabinet, and laboratory access was restricted to a single operator during sample processing to minimize airborne particle contamination.

ACCEPTED

Development and Evaluation of the MP Extraction Workflow

Reliable fluorescence-based detection of MPs in animal feed requires efficient removal of matrix-derived organic constituents while preserving the measurable fluorescence responses of reference polymer particles. Therefore, an extraction workflow combining TMAH digestion with TCM extraction prior to NR staining was developed and evaluated. The workflow was designed to reduce proteins, lipids, pigments, and other organic constituents that may interfere with fluorescence analyses while preserving the fluorescence response of particles. The overall experimental workflow is illustrated in **Figure 1**. The proposed workflow was subsequently evaluated using individual reference polymer particles, PolyMix, fortified feed, and feed samples to assess whether the fluorescence responses of the reference polymer particles were preserved following sample preparation.

Digestion of Organic Matter and MP Extraction

Approximately 0.50 g of each feed or fortified feed sample was transferred into 15-mL borosilicate glass tube, followed by the addition of 5 mL TMAH. Samples were vortexed and incubated at 60 °C under continuous shaking (200 rpm) for 24 h to facilitate digestion of organic matter (25).

Following digestion, 10 mL TCM was added, and the suspensions were centrifuged at 4000 rpm for 10 min. The washing procedure was repeated three times using fresh TCM, with vortex mixing before each centrifugation step. After the third washing cycle, an additional 10 mL of TCM was added, and the samples were incubated again at 60 °C with shaking (200 rpm) for 1 h to remove residual lipophilic organic compounds.

The suspensions were subsequently centrifuged at 4000 rpm for 10 min and subjected to vacuum filtration. To minimize polymer loss during extraction, all TCM fractions collected throughout the washing procedure were filtered through the same membrane filter. In contrast, the TMAH digestion solution was not filtered because it primarily contained dissolved organic constituents rather than intact polymer particles.

Nile Red Staining and Fluorescence Microscopy

Nile Red ($C_{20}H_{18}N_2O_2$) staining was performed according to the method described by Shim et al. (2016) (26). Briefly, NR was dissolved in acetone and subsequently diluted with *n*-hexane to obtain a final concentration of 5 mg L^{-1}. An aliquot of 1 mL of the staining solution was applied to each filter to ensure complete surface coverage and incubated at room temperature for 20 min. Following staining, the filters were rinsed with filtered distilled water using a vacuum filtration system to remove excess dye. The filters were then dried at 50 °C for 30 min, transferred to clean glass Petri dishes, covered with aluminum foil to minimize photobleaching, and stored until microscopic examination.

ACCEPTED

Fluorescence imaging was performed using a fluorescence microscope (BAB, Türkiye) equipped with a blue excitation filter as described by Yurtsever and Cuevelek (2024) (27). All images were acquired using identical microscope settings, including magnification, exposure conditions, excitation filter, and camera parameters, to ensure direct comparison of fluorescence responses among the experimental groups. No brightness or contrast adjustments were applied to the images before fluorescence intensity analysis.

Fluorescence Intensity Analysis

Fluorescence images were analyzed using ImageJ Software (National Institutes of Health, USA). Mean fluorescence intensity was determined from Regions of Interest (ROI) corresponding to individual fluorescent polymer particles. Reference polymer particles were first analyzed individually to establish the characteristic fluorescence response of each polymer. The same analytical procedure was subsequently applied to PolyMix, Fortified-feed, and feed samples following extraction and NR staining. Fluorescence intensity values obtained from the individual reference polymers were used as baseline values for comparison with the corresponding reference polymers in PolyMix, fortified-feed, and feed conditions.

The resulting fluorescence intensity data were used to evaluate whether the proposed extraction workflow preserved the fluorescence responses of the reference polymer particles after sample preparation. Furthermore, fluorescence intensity measurements were subjected to statistical analysis and discriminant function analysis to assess their potential as a complementary analytical parameter for preliminary polymer differentiation.

Statistical Analysis

Statistical analyses were performed using IBM SPSS Statistics version 23 (IBM Corp., Armonk, NY, USA). Data were initially evaluated for normality using the Shapiro-Wilk test. Differences in fluorescence intensity among polymer types were assessed using one-way analysis of variance (ANOVA) for normally distributed data, whereas the Kruskal-Wallis test was applied when the assumption of normality was not satisfied.

Linear regression analysis was performed to evaluate the agreement between observed and predicted fluorescence intensity values. Model assumptions were assessed using normal probability (P-P) plot of standardized residuals, whereas influential observations were evaluated using Cook's distance.

Finally, Discriminant Function Analysis (DFA) was performed to evaluate the ability of fluorescence intensity to differentiate among the reference polymer types. Statistical significance was accepted at $p<0.05$.

Results

ACCEPTED

Fluorescence microscopy performed under blue-light excitation demonstrated that the proposed TMAH-TCM extraction workflow reduced matrix-derived fluorescence interference while preserving detectable fluorescence signals from polymer particles following NR staining. Following extraction, polymer particles exhibited clear fluorescence signals with minimal background interference, allowing both qualitative evaluation of fluorescence color and quantitative measurement of fluorescence intensity (**Figures 2-8**).

Preservation of Polymer Fluorescence Following Extraction

The fluorescence responses of PE, PP, PS, and PET were evaluated throughout the analytical workflow by comparing individual reference polymer particles, PolyMix, fortified feed, and feed samples (**Table 3**). No significant differences in fluorescence intensity were observed among the corresponding experimental groups for PE ($p=0.937$), PP ($p=0.998$), PS ($p=1.000$), and PET ($p=0.932$). These findings indicate that the measured fluorescence responses of the reference polymers were largely preserved throughout sample preparation.

Linear regression diagnostics further supported the robustness of the analytical workflow. Cook's distance values remained below the threshold of 1 for all regression models, indicating the absence of influential observations and confirming the stability of fluorescence intensity measurements across all experimental groups (**Figures 2A-5A´**).

Fluorescence Characteristics of Polymer Particles

Following NR staining, the four polymer types exhibited distinct fluorescence colors and fluorescence intensities under identical imaging conditions (**Figures 6 and 7**). Visual differences in fluorescence color provided qualitative information on the fluorescence characteristics of the polymer particles, whereas fluorescence intensity was quantitatively measured for statistical comparison among polymer types.

Overall, fluorescence intensity differed significantly among the four polymers ($p<0.05$) (**Table 3**). Polystyrene exhibited the highest fluorescence intensity (174.69 ± 20.91), followed by PP (143.21 ± 37.74), PE (134.03 ± 38.36), and PET (117.59 ± 36.93). Pairwise comparisons revealed no significant differences between PE and PP ($p=0.270$) or between PE and PET ($p=0.172$). In contrast, significant differences were observed between PP and PS ($p=0.002$), PP and PET ($p=0.021$), PE and PS ($p<0.001$), and PS and PET ($p<0.001$).

Collectively, qualitative fluorescence color observations and quantitative fluorescence intensity measurements provided complementary information on the fluorescence characteristics of the reference polymer particles.

Polymer Differentiation Based on Fluorescence Intensity

Discriminant function analysis (DFA) was performed to evaluate whether fluorescence intensity could discriminate among the four polymer types. The analysis demonstrated significant discrimination among polymer groups (Wilk's

ACCEPTED

λ=0.660, $p<0.001$). The canonical correlation (0.583) and eigenvalue (0.515) indicated moderate discriminatory performance of the model. Group centroids showed that PS (1.023) was the most distinct polymer, followed by PP (0.074), PE (-0.204), and PET (-0.775) (**Figure 8**).

Overall classification accuracy reached 47.3%, remaining virtually unchanged after cross-validation (47.0%). Misclassification occurred primarily among the polymer groups, with 40.8% of PP particles classified as PS and 37.5% of PET particles classified as PE. Although the discriminant function was statistically significant, the cross-validated classification accuracy of 47.0% indicated only moderate discriminatory performance and substantial overlap among some polymer groups. Therefore, fluorescence intensity alone was insufficient for definitive polymer identification and should be interpreted as complementary quantitative information for preliminary polymer differentiation rather than as a stand-alone identification parameter.

Removal of Matrix-Derived Interference

Following TMAH-TCM treatment and NR staining, fluorescence microscopy revealed NR-positive particles in the non-fortified feed samples with relatively low background fluorescence (**Table 4**). Some particles exhibited fluorescence characteristics similar to those observed for the reference polymers. However, because polymer identity was not independently confirmed by spectroscopic analysis, these particles were not definitively assigned to specific polymer types.

ACCEPTED

Discussion

Challenges of Using Nile Red Dye in Microplastic Research

Nile Red is a lipophilic fluorescent dye that selectively binds to hydrophobic materials, making it one of the most widely used staining agents for the detection of MPs in complex environmental and biological matrices (26). Galvao et al. (2022) demonstrated that NR produces substantially stronger fluorescence than unstained polymer particles, enabling rapid visualization and facilitating high-throughput fluorescence microscopy (28). These characteristics make NR particularly attractive for screening large numbers of environmental and biological samples using fluorescence microscopy. Despite these advantages, the lipophilic nature of NR also represents one of its major limitations. In addition to plastic particles, NR readily binds to lipids and other hydrophobic organic constituents that are abundant in biological matrices such as animal feeds. Consequently, residual organic matter may produce false-positive fluorescence signals, compromising the specificity and reliability of MP identification (29,30). This limitation highlights the importance of efficient sample pretreatment to remove matrix-derived organic compounds before

staining (31). Hydrogen peroxide (H_2O_2) and potassium hydroxide (KOH) are widely employed for this purpose because of their ability to digest biological residues and improve the specificity of NR staining (1). However, although TCM is well recognized for its excellent lipid-solubilizing capacity, it has received comparatively little attention as an extraction solvent in MP studies (32). Considering that animal feeds are particularly rich in lipids and other hydrophobic constituents, incorporating TCM into the extraction workflow may provide an important advantage by removing compounds that would otherwise compete with MPs for NR binding.

Another important consideration is that prolonged exposure to alkaline reagents may modify the surface properties of certain polymers, particularly PET, thereby influencing NR adsorption and fluorescence behavior (33). Therefore, the development of an extraction protocol should reduce organic matter interference while preserving the fluorescence characteristics of polymer particles required for subsequent NR-based analysis.

The interaction between NR and polymer particles is also polymer dependent. Aoki et al. (2022) reported that PP exhibited the highest fluorescence intensity following NR staining (34). In contrast, PS produced the strongest fluorescence response in the present study. Rather than representing contradictory findings, these differences likely reflect variations in particle preparation, particle morphology, surface oxidation, staining conditions, and analytical workflows, all of which are known to influence NR fluorescence. Consequently, fluorescence intensity should be interpreted within the context of the analytical protocol employed rather than as an absolute polymer-specific characteristic.

In addition to polymer composition, NR fluorescence may also be influenced by experimental factors including pH, temperature, and the presence of residual organic compounds (28). Standardization of staining conditions is therefore essential for obtaining reproducible fluorescence measurements. Furthermore, additives and pigments incorporated during plastic manufacturing may influence fluorescence responses by altering dye adsorption (35). This was relevant for the PS reference particles used in the present study, which were prepared from commercially available black plastic lids. The dark carbon-based pigments initially present on the particle surface could potentially interfere with fluorescence measurements. Following TCM extraction, an apparent reduction in the dark pigmentation of PS particles was visually observed (**Figure 9**). However, because pigment removal was not quantitatively measured and the surface integrity of PS was not independently characterized before and after TCM exposure, the observed fluorescence response cannot be attributed solely to pigment removal, and a potential contribution of solvent – polymer interactions cannot be excluded.

Development and Evaluation of the MP Extraction Workflow

ACCEPTED

The primary objective of the proposed workflow was to reduce matrix-derived organic interference while preserving the fluorescence characteristics of polymer particles required for subsequent NR-based analysis. Fluorescence microscopy showed low background fluorescence following TMAH-TCM treatment, while clear fluorescence signals from the reference polymer particles remained detectable. Furthermore, the absence of significant differences in fluorescence intensity among the corresponding individual polymer, PolyMix, fortified- feed, and feed conditions indicated that the fluorescence responses of the tested reference polymers were largely preserved throughout sample preparation. Taken together, these observations suggest that the proposed workflow can facilitate NR-based screening of MPs in complex animal feed matrices by reducing matrix-associated fluorescence interference without substantially altering the measured fluorescence responses of the tested polymers.

The effectiveness of the extraction protocol can be explained by the complementary roles of TMAH and TCM. TMAH has been widely applied for digestion of organic-rich matrices because it efficiently degrades proteins and other biological constituents while minimizing damage to polymer particles (36). TMAH (25 wt. % in methanol) has a density of approximately 1.00 g cm^{-3} between 50 and 70 °C (37), which reduces the likelihood of losing low-density polymers such as PE and PP during centrifugation. Elevated temperatures further enhance the digestion efficiency of TMAH by increasing the solubility of organic constituents, thereby improving sample purification before fluorescence analysis (25).

Following digestion, TCM served as the extraction solvent because of its strong affinity for lipids and other hydrophobic compounds commonly present in animal feeds. Although dichloromethane (DCM) has previously been used for similar applications (36), TCM was selected in the present study based on its lipid-solubilizing properties and physicochemical characteristics. First, its greater lipid-solubilizing capacity may facilitate the removal of compounds that could otherwise interfere with NR staining (38). Second, its higher boiling point (61.2 °C) compared with DCM (39.6 °C) may reduce solvent evaporation during extraction at elevated temperatures and thereby contribute to more stable extraction conditions (39). These characteristics make TCM particularly suitable for lipid-rich feed matrices, where efficient removal of hydrophobic residues is essential for reducing background fluorescence.

The density of the extraction solvent also influences polymer behavior during centrifugation. Owing to their relatively low densities, PE (0.89-0.98 g cm^{-3}) and PP (0.85-0.92 g cm^{-3}) tend to remain suspended in dense solvents rather than precipitating (40). With a density of approximately 1.47 g cm^{-3}, TCM provides a denser extraction medium than DCM (1.30 g cm^{-3}) (41), which may favor the retention of low-density polymers in the supernatant during extraction and potentially reduce polymer loss before filtration.

ACCEPTED

Quantitative recovery and precision were not assessed in the present study. Because the reference polymer particles were prepared from commercial plastic products and were heterogeneous in size and morphology, a known particle number could not be reliably established for calculation of particle-based recovery rates. The present evaluation therefore focused on whether fluorescence responses were preserved across the analytical workflow by comparing individual reference polymer particles, PolyMix, fortified-feed, and feed conditions. The absence of significant differences in fluorescence intensity among the corresponding conditions indicated that the measured fluorescence responses of the tested reference polymers were largely preserved during sample preparation. Nevertheless, quantitative recovery (%) and precision (RSD%) remain necessary for full analytical validation of the proposed workflow and should be addressed in future studies using well-characterized particles with known particle numbers.

Fluorescence Characteristics as a Complementary Tool for Polymer Differentiation

The present study demonstrated that the proposed TMAH-TCM extraction workflow effectively preserved the fluorescence characteristics of reference polymer particles following NR staining. Although fluorescence microscopy is primarily used for rapid visualization of MPs, the present findings indicate that fluorescence characteristics may also provide complementary information for preliminary differentiation among polymer types after appropriate sample preparation.

Among the four polymers evaluated, PS exhibited the highest fluorescence intensity and differed significantly from PE, PP, and PET ($p<0.001$ for PE and PET; $p=0.002$ for PP). In contrast, no significant differences were observed between PE and PP or between PE and PET. However, the moderate cross-validated DFA accuracy (47.0%) and the observed misclassification among polymer groups demonstrate substantial overlap in fluorescence intensity distributions. Therefore, fluorescence intensity should not be considered a stand-alone parameter for polymer identification but rather complementary quantitative information for preliminary polymer differentiation. Definitive polymer identification requires confirmation using polymer-specific analytical techniques such as FTIR or Raman spectroscopy.

The higher fluorescence intensity observed for PS differs from the findings of Aoki (2022), who reported PP as the polymer exhibiting the strongest NR fluorescence (34). However, this discrepancy is unlikely to represent a true contradiction because NR fluorescence can be influenced by particle morphology, surface oxidation, staining conditions, extraction procedures, and imaging protocols. Unlike the relatively uniform polymer particles used by Aoki (2022), the particles prepared in the present study originated from commercially available plastic products and therefore exhibited heterogenous sizes and surface characteristics. Consequently, differences in fluorescence behavior

ACCEPTED

among studies are expected and highlight the importance of interpreting fluorescence responses within the context of the applied analytical workflow.

The fluorescence behavior of PS may also be explained by its chemical structure. PS contains aromatic rings that facilitate π-π interactions with the aromatic structure of NR, thereby enhancing dye adsorption onto the polymer surface (42). In addition, the crushing and pulverization procedures used during particle preparation may have increased surface roughness and surface oxidation, creating additional adsorption sites for the dye. Together, these characteristics may explain the stronger fluorescence observed for PS particles following extraction and staining. However, this interpretation should be considered cautiously because chloroform may interact with PS and potentially alter its surface characteristics. Since polymer surface integrity was not independently characterized before and after TCM exposure, the present study cannot determine whether the observed PS fluorescence response was influenced, at least in part, by solvent-polymer interactions.

In contrast, PET exhibited substantially lower fluorescence intensity despite also containing aromatic rings. This observation may be explained by the semi-crystalline structure of PET, which consists of densely packed polymer chains that reduce dye penetration into the polymer matrix. Furthermore, PET contains fewer accessible π-electron systems than PS (15), potentially limiting the interaction between NR and the polymer surface. Similarly, PP exhibited only slightly greater fluorescence intensity than PE, although this difference was not statistically significant. Because the methyl side groups present in PP are not expected to interact directly with NR, the small increase in fluorescence intensity is more likely associated with subtle differences in surface properties that influence dye adsorption rather than with fundamental differences in polymer chemistry.

Overall, the present findings demonstrate that effective removal of matrix-derived organic interference allows the fluorescence characteristics of reference polymer particles to be preserved following NR staining. Consequently, the combined evaluation of fluorescence color and fluorescence intensity provides complementary information for preliminary polymer differentiation in complex animal feed matrices. Although spectroscopic techniques remain essential for definitive polymer identification, the proposed workflow offers a rapid screening strategy that may enhance the efficiency of MP analysis in agricultural samples.

ACCEPTED

Acknowledgments

The author sincerely thanks Dr. Meral Yurtsever for providing access to the laboratory facilities and for her valuable comments on an earlier version of the manuscript.

References

1. Malla-Pradhan R, Phoungthong K, Suwunwong T, Joshi TP, Pradhan BL. Microplastic pollution in lakeshore sediments: the first report on abundance and composition of Phewa Lake, Nepal. Environ Sci Pollut Res. 2023;30(27):70065–75.
2. Yang L, Zhang Y, Kang S, Wang Z, Wu C. Microplastics in soil: A review on methods, occurrence, sources, and potential risk. Sci Total Environ. 2021;780:146546.
3. Okoffo ED, O'Brien S, Ribeiro F, Burrows SD, Toapanta T, Rauert C, et al. Plastic particles in soil: state of the knowledge on sources, occurrence and distribution, analytical methods and ecological impacts. Environ Sci Process Impacts. 2021;23(2):240–74.
4. Dong X, Liu X, Hou Q, Wang Z. From natural environment to animal tissues: A review of microplastics(nanoplastics) translocation and hazards studies. Sci Total Environ. 2023 Jan;855:158686.
5. Patrucco SG, Abid K, Rivoira L, Bruzzoniti MC, Bracco P, Kaihara H, et al. Microplastics contamination in ruminant feeds of Northwestern Italy: a preliminary assessment. Sci Total Environ. 2025;1001:180479.
6. Urbina MA, Correa F, Aburto F, Ferrio JP. Adsorption of polyethylene microbeads and physiological effects on hydroponic maize. Sci Total Environ. 2020;741:140216.
7. Tamargo A, Molinero N, Reinosa JJ, Alcolea-Rodriguez V, Portela R, Bañares MA, et al. PET microplastics affect human gut microbiota communities during simulated gastrointestinal digestion, first evidence of plausible polymer biodegradation during human digestion. Sci Rep. 2022 Jan 11;12(1):528.
8. Saha SC, Saha G. Effect of microplastics deposition on human lung airways: A review with computational benefits and challenges. Heliyon. 2024 Jan;10(2):e24355.
9. Hou B, Wang F, Liu T, Wang Z. Reproductive toxicity of polystyrene microplastics: In vivo experimental study on testicular toxicity in mice. J Hazard Mater. 2021;405:124028.
10. Wang M, Wu Y, Li G, Xiong Y, Zhang Y, Zhang M. The hidden threat: Unraveling the impact of microplastics on reproductive health. Sci Total Environ. 2024 Jul;935:173177.
11. Chang X, Li Y, Han Y, Fang Y, Xiang H, Zhao Z, et al. Polystyrene exposure induces lamb gastrointestinal injury, digestive disorders and inflammation, decreasing daily gain, and meat quality. Ecotoxicol Environ Saf. 2024 Jun;277:116389.

ACCEPTED

12. Lee Y, Cho J, Sohn J, Kim C. Health Effects of Microplastic Exposures: Current Issues and Perspectives in South Korea. Yonsei Med J. 2023;64(5):301.

13. Levermore JM, Smith TEL, Kelly FJ, Wright SL. Detection of microplastics in ambient particulate matter using Raman spectral imaging and chemometric analysis. Anal Chem. 2020;92(13):8732–40.

14. Nakano R, Gürses RK, Tanaka Y, Ishida Y, Kimoto T, Kitagawa S, et al. Pyrolysis-GC–MS analysis of ingested polystyrene microsphere content in individual Daphnia magna. Sci Total Environ. 2022;817:152981.

15. Jin MY, Zhen Q, Xiao D, Tao G, Xing X, Yu P, et al. Engineered non-covalent π interactions as key elements for chiral recognition. Nat Commun. 2022 Jun 7;13(1):3276.

16. Nelms SE, Barnett J, Brownlow A, Davison NJ, Deaville R, Galloway TS, et al. Microplastics in marine mammals stranded around the British coast: ubiquitous but transitory? Sci Rep. 2019;9(1):1075.

17. Stanton T, Johnson M, Nathanail P, Gomes RL, Needham T, Burson A. Exploring the efficacy of Nile red in microplastic quantification: A costaining approach. Environ Sci Technol Lett. 2019;6(10):606–11.

18. Helmberger MS, Auscavitch S, Linehan J, Shank TM, Cordes E, Rotjan RD. Microplastic accumulation visually and fluorescently undetectable within deepwater corals of the remote equatorial Pacific. Deep Sea Res Part I Oceanogr Res Pap. 2025;223:104550.

19. Majcen A, Tassoti S, Spitzer P. Lighting up for learning─ fluorescence analysis of microplastic particles by secondary school students using Nile Red. J Chem Educ. 2023;100(10):4007–12.

20. Macairan JR, Nguyen B, Li F, Tufenkji N. Tissue clearing to localize microplastics via three-dimensional imaging of whole organisms. Environ Sci Technol. 2023;57(23):8476–83.

21. Michler-Kozma DN, Kruckenfellner L, Heitkamp A, Ebke KP, Gabel F. Uptake and transfer of polyamide microplastics in a freshwater mesocosm study. Water. 2022;14(6):887.

22. Glorio Patrucco S, Rivoira L, Bruzzoniti MC, Barbera S, Tassone S. Development and application of a novel extraction protocol for the monitoring of microplastic contamination in widely consumed ruminant feeds. Sci Total Environ. 2024 Oct;947:174493.

23. Özgenç E. Advanced analytical techniques for assessing and detecting microplastic pollution in water and wastewater systems. Environ Qual Manag. 2024 Sep 11;34(1).

24. Meng X, Zheng X, Mai W, Gao J, Fan Y, Fu J, et al. Micro-and nanoplastics differ in particle-mucus interactions: The sight on rheological properties, barrier dysfunction and microbiota dysbiosis. J Hazard Mater. 2025;492:138130.

ACCEPTED

25. Cerqueira UMFM, Alves JPS, Santos WNL, da Silva Pita B, Novaes CG, Araújo SA, et al. Recent applications of tetramethylammonium hydroxide (TMAH) in the sample preparation for elemental analysis by spectroanalytical techniques. Adv Sample Prep. 2024 Feb;9:100104.

26. Shim WJ, Song YK, Hong SH, Jang M. Identification and quantification of microplastics using Nile Red staining. Mar Pollut Bull. 2016 Dec;113(1–2):469–76.

27. Yurtsever M, Cuevelek MA. Abundance of microplastics in the agro-industrial product beet sugar; food or plastifood. Process Saf Environ Prot. 2024;188:467–79.

28. Galvao LS, Ferreira RR, Fernandes EMS, Correia CA, Valera TS, dos Santos Rosa D, et al. Analysis of selective fluorescence for the characterization of microplastic fibers: use of a Nile Red-based analytical method to compare between natural and synthetic fibers. J Hazard Mater. 2023;443:130217.

29. Kang H, Park S, Lee B, Ahn J, Kim S. Modification of a Nile Red Staining Method for Microplastics Analysis: A Nile Red Plate Method. Water. 2020 Nov 19;12(11):3251.

30. Michelaraki M, Joseph O, Karnik S, Devalla S, Madanan K, Prabhu R. Potential for Nile red dye-based analysis of microplastics from oceanic samples. In: Global Oceans 2020: Singapore–US Gulf Coast. IEEE; 2020. p. 1–4.

31. Prata JC, Alves JR, da Costa JP, Duarte AC, Rocha-Santos T. Major factors influencing the quantification of Nile Red stained microplastics and improved automatic quantification (MP-VAT 2.0). Sci Total Environ. 2020 Jun;719:137498.

32. Li Y, Ghasemi Naghdi F, Garg S, Adarme-Vega T, Thurecht KJ, Ghafor W, et al. A comparative study: the impact of different lipid extraction methods on current microalgal lipid research. Microb Cell Fact. 2014;13(1):14.

33. Pfeiffer F, Fischer EK. Various Digestion Protocols Within Microplastic Sample Processing—Evaluating the Resistance of Different Synthetic Polymers and the Efficiency of Biogenic Organic Matter Destruction. Front Environ Sci. 2020 Dec 23;8.

34. Aoki H. Material-Specific Determination Based on Microscopic Observation of Single Microplastic Particles Stained with Fluorescent Dyes. Sensors. 2022 Apr 28;22(9):3390.

35. Prata JC. Influence of intrinsic plastics characteristics on Nile Red staining and fluorescence. J Sea Res. 2023;195:102431.

36. Li P, Lai Y, Zheng R gang, Li Q cun, Sheng X, Yu S, et al. Extraction of common small microplastics and

ACCEPTED

nanoplastics embedded in environmental solid matrices by tetramethylammonium hydroxide digestion and dichloromethane dissolution for Py-GC-MS determination. Environ Sci Technol. 2023;57(32):12010–8.

37. Diebold J, Weiß Y, Zürcher S, Schmidt MS. Dataset for density/temperature correlation of tetramethylammonium hydroxide solutions of various concentrations. Data Br. 2022 Dec;45:108679.

38. Saini RK, Prasad P, Shang X, Keum YS. Advances in Lipid Extraction Methods—A Review. Int J Mol Sci. 2021 Dec 20;22(24):13643.

39. Pecorini G, Braccini S, Simoni S, Corti A, Parrini G, Puppi D. Additive Manufacturing of Wet-Spun Poly(3-hydroxybutyrate- *co* -3-hydroxyvalerate)-Based Scaffolds Loaded with Hydroxyapatite. Macromol Biosci. 2024 Jun 3;24(6).

40. Erni-Cassola G, Zadjelovic V, Gibson MI, Christie-Oleza JA. Distribution of plastic polymer types in the marine environment; A meta-analysis. J Hazard Mater. 2019 May;369:691–8.

41. Zhang HL. Viscosity and Density for Binary Mixtures of Carbon Tetrachloride + Chloroform, Carbon Tetrachloride + Dichloromethane, and Chloroform + Dichloromethane and One Ternary Mixture of Chloroform + 1:1 (Carbon Tetrachloride + Dichloromethane) at 303.15 K. J Chem Eng Data. 2003 Jan 1;48(1):52–5.

42. Woo H, Kang SH, Kwon Y, Choi Y, Kim J, Ha DH, et al. Sensitive and specific capture of polystyrene and polypropylene microplastics using engineered peptide biosensors. RSC Adv. 2022;12(13):7680–8.

43. Grigorescu RM, Grigore ME, Iancu L, Ghioca P, Ion RM. Waste Electrical and Electronic Equipment: A Review on the Identification Methods for Polymeric Materials. Recycling. 2019 Aug 13;4(3):32.

44. Bouwman H, Minnaar K, Bezuidenhout C, Verster C. Microplastic in freshwater environments-A scoping study. Pretoria Water Res Comm. 2018;

ACCEPTED

Tables and Figures

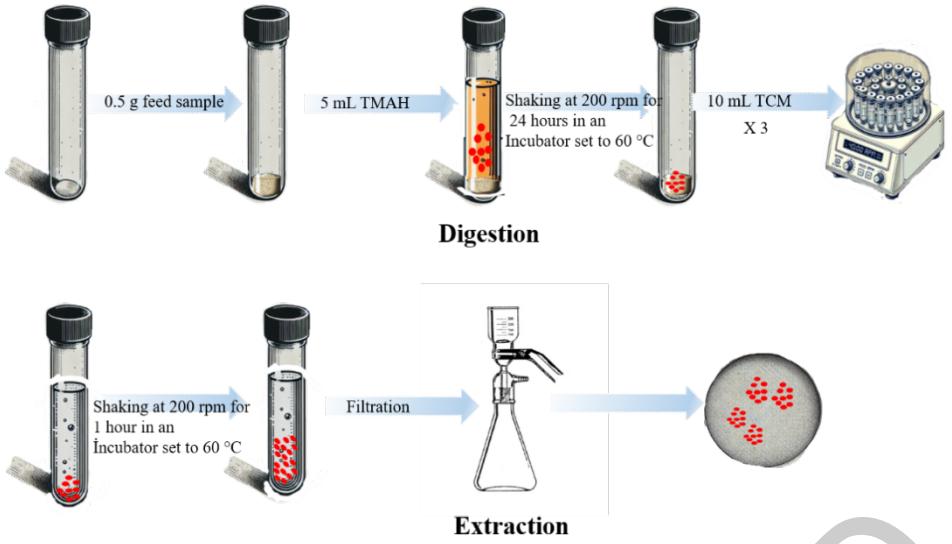
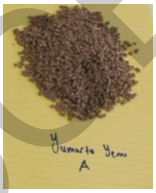
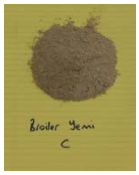


Figure 1. MPs extraction procedures

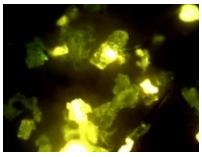
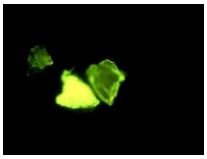
Table 1. Feed samples which are commonly used in different farm animals. All pelleted form was pulverized in a grinder to obtain particles under the 125 µm in size. A feed sample was randomly chosen to spike (fortified) with MPs. All feed samples were extracted.

Feed Materials	Particle Size		
	3-6 mm	≤ 600 µm	≤ 125 µm
Layer Feed			
Calf Starter Feed			
Broiler Feed			
Calf Grower Feed			

ACCEPTED

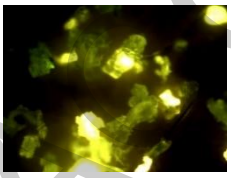
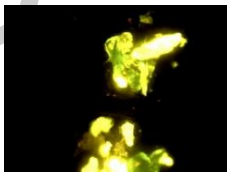
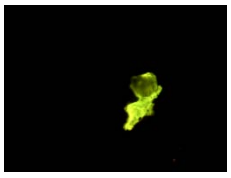
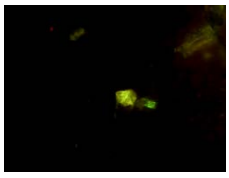
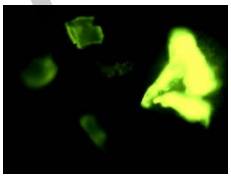
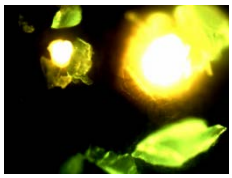
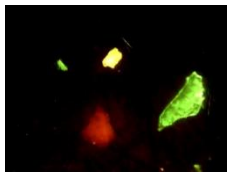
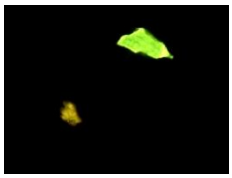
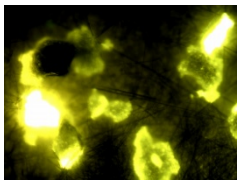
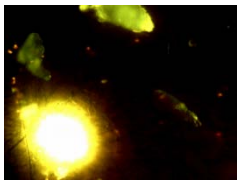
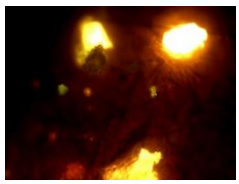
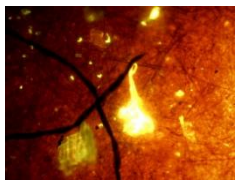
Turkey Feed			

Table 2. Plastic polymers obtained from single-used commercial products.

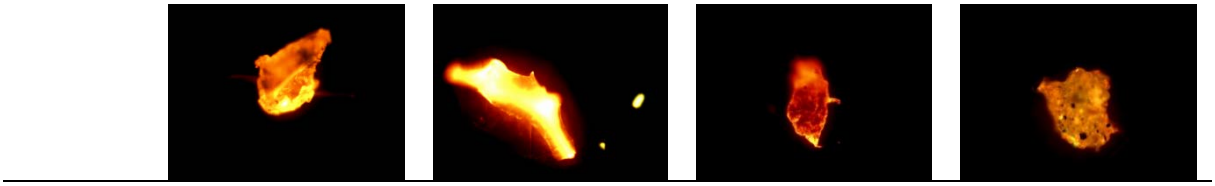
Polymer Type	**Density (g/cm^3)** (43,44)	**Origin**	**Length range (µm)**	**Original Image**	**Fluorescent Images (Original)**
PE	0.91-0.97	Bubble wrap	4.4-114.8 µm		
PP	0.87-0.92	Plastic pencil case	2.8-103.6 µm		
PS	1.04-1.08	Plastic plate and lid	9.2-122.4 µm		
PET	1.38-1.41	Plastic bottle	6-125.4 µm		

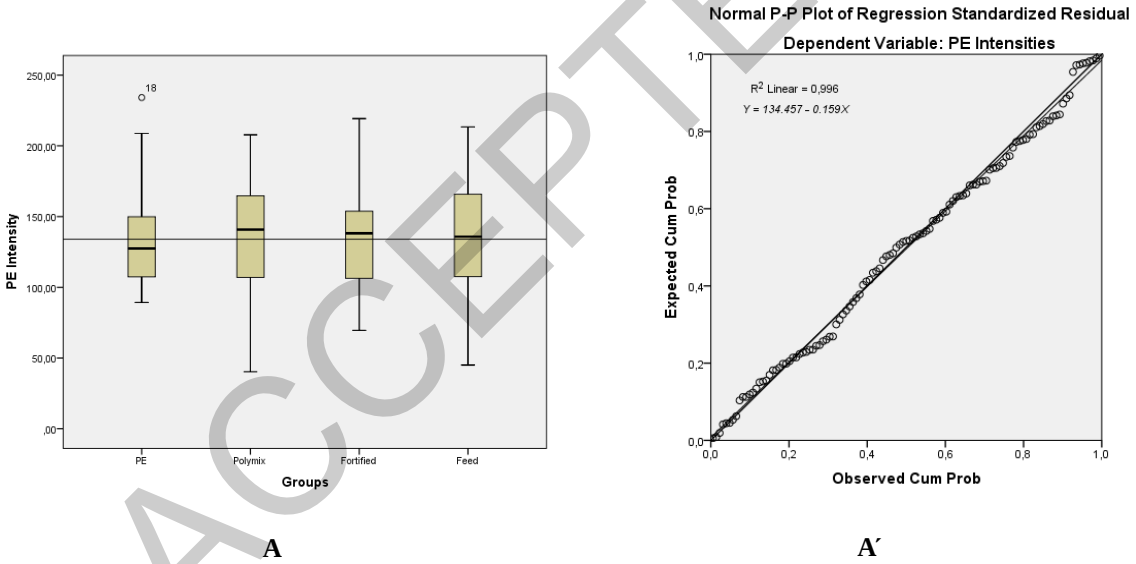
ACCEPTED

Table 3. The mean fluorescent intensity of polymers (PE, PP, PS, and PET) and polymers within the feed matrices. Different superscript letters in the same column refer to mean values statistically different according to the Kruskal-Wallis ($p < 0.05$). According to the post hoc pairwise comparison using the Mann-Whitney U test; means of PE and PP groups showed no significant differences ($p = 0.270$); PP and PS groups exhibited significant differences ($p = 0.002$); PP and PET groups also showed a significant difference ($p = 0.021$); a significant difference was also observed between PE and PS groups ($p < 0.001$); PE and PET groups exhibited no significant difference ($p = 0.172$). Conversely, common letters in the same column and rows refer to mean fluorescence not statistically different from one to other according to the Kruskal-Wallis and one way ANOVA (significance threshold level 0.05).

	Polymers	**Polymix**	**Fortified**	**Feed**
	134.03±38.36^{ab}	134.98±51.67^{ab}	133.90±31.26^{ab}	133.81±39.49^{ab}
PE				
	143.21±37.74^{b}	143.91±45.68^{b}	145.43±33.78^{b}	144.65±31.94^{b}
PP				
	174.69±20.91^{c}	174.62±19.39^{c}	174.60±29.40^{c}	174.40±27.13^{c}
PS				
PET	117.59±36.93^{ad}	116.27±37.19^{ad}	116.91±28.73^{ad}	116.23±25.35^{ad}

ACCEPTED

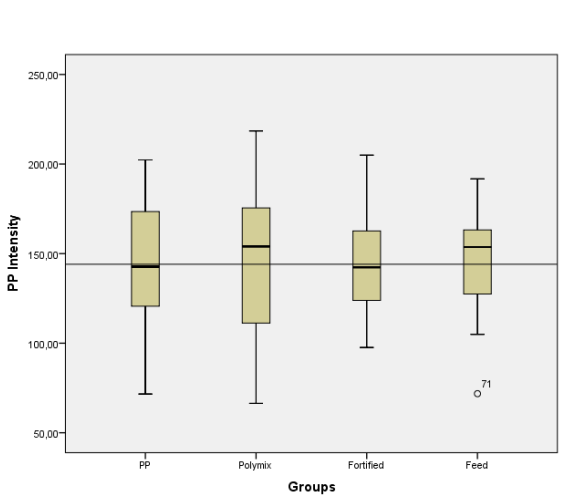




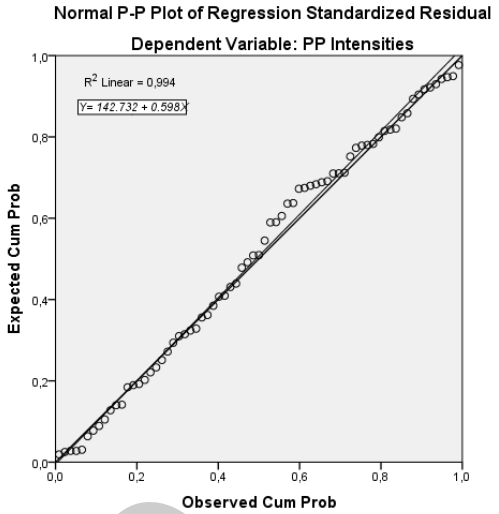
A **A´**

ACCEPTED

Figure 2. Comparison of PE polymer's fluorescent intensities across the different groups (Individual polymers, Polymix, Fortified, and Feed) and the impact of individual intensity observations on the overall model (All Cook's Distance values were significantly below the threshold level of 1 [0.000]).



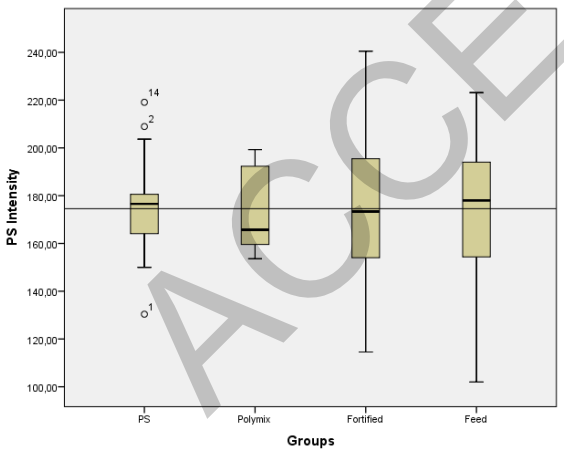
A



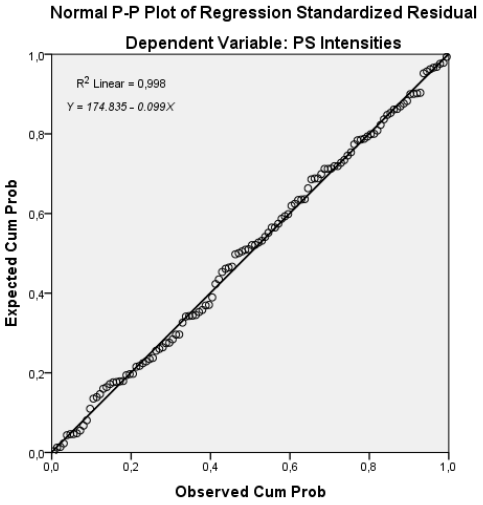
A´

Figure 3. Comparison of PP polymer's fluorescent intensities across the different groups (Individual polymers, Polymix, Fortified, and Feed) and the impact of individual intensity observations on the overall model (All Cook's Distance values were significantly below the threshold level of 1 [0.000]).

ACCEPTED

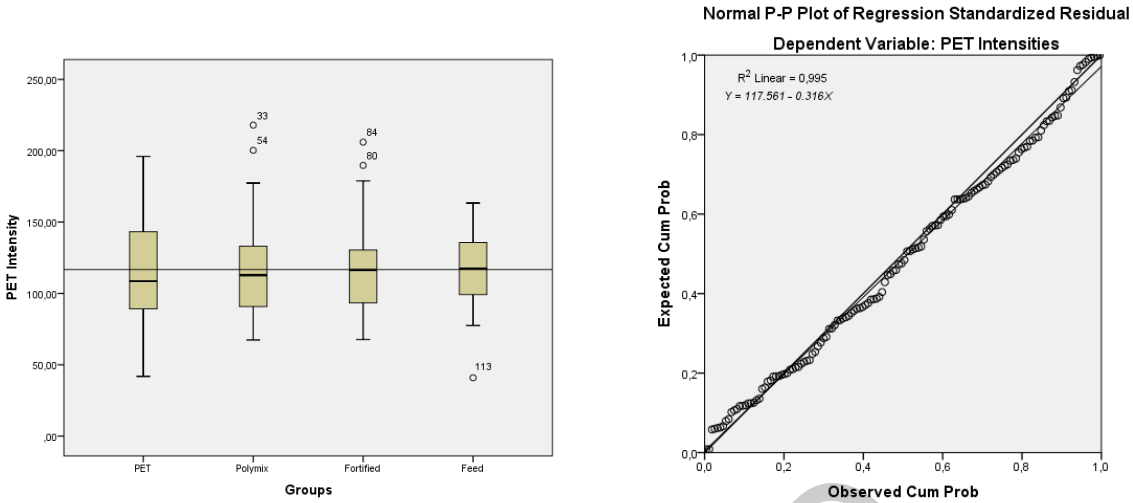


A



A´

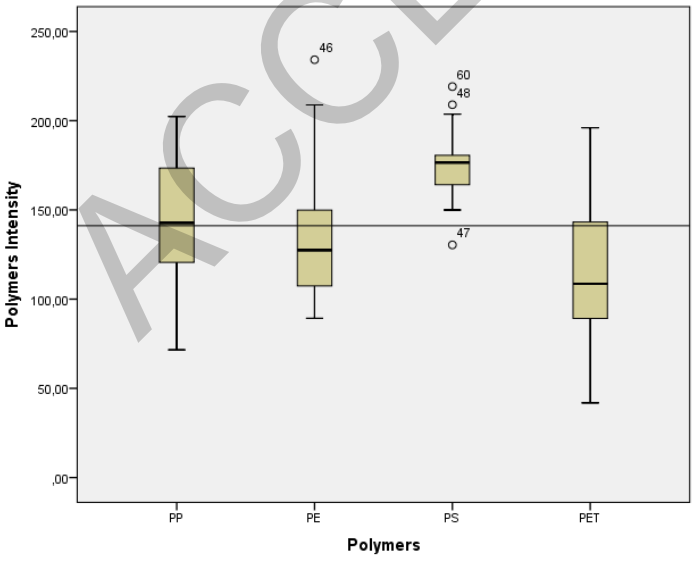
Figure 4. Comparison of PS polymer's fluorescent intensities across the different groups (Individual polymers, Polymix, Fortified, and Feed) and the impact of individual intensity observations on the overall model (All Cook's Distance values were significantly below the threshold level of 1 [0.000]).



A **A´**

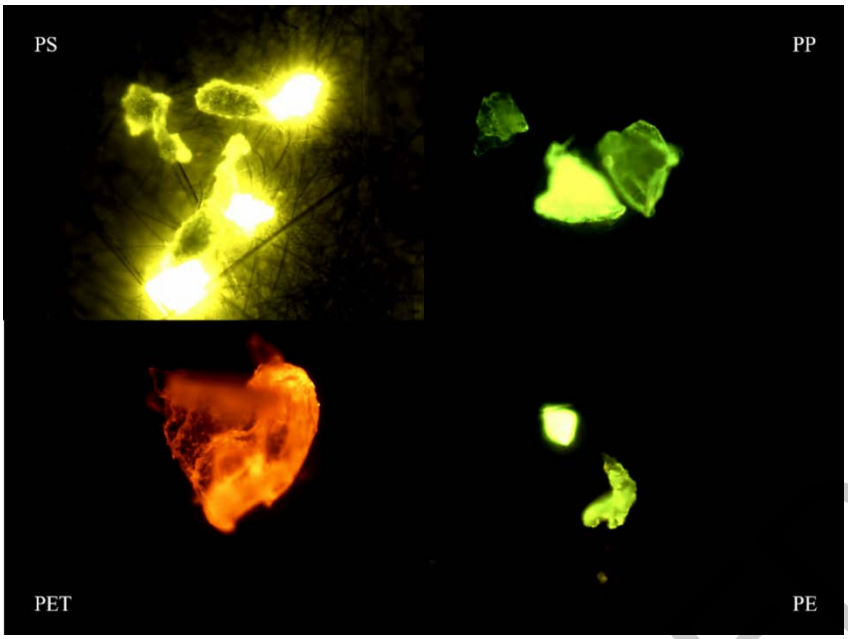
Figure 5. Comparison of PET polymer's fluorescent intensities across the different groups (Individual polymers, Polymix, Fortified, and Feed) and the impact of individual intensity observations on the overall model (All Cook's Distance values were significantly below the threshold level of 1 [0.000]).

ACCEPTED



Kruskal-Wallis test revealed statistically significant differences between the individual polymers ($p < 0.05$).
According to Mann-Whitney U test; no significant differences between the PE and PP groups ($p = 0.270$); PP and PS groups exhibited significant differences ($p = 0.002$); PP and PET groups also showed a significant difference ($p = 0.021$); a significant difference was also observed between PE and PS groups ($p < 0.001$), PE and PET groups exhibited no significant difference ($p = 0.172$); finally PS and PET showed a significant difference ($p < 0.001$).

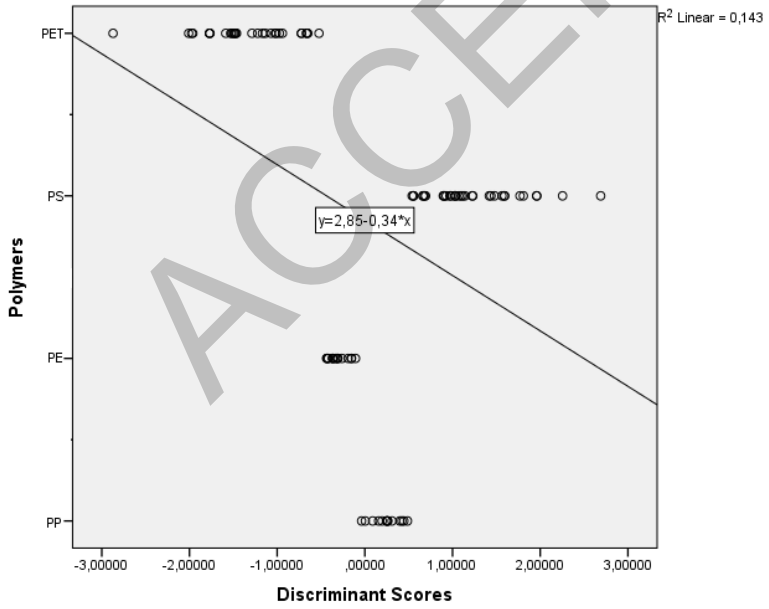
Figure 6. Boxplot of individual polymers's fluorescence intensities highlighting variance within the groups for PE, PP, PS, and PET.



Fluorescence imaging of different polymers stained with NR under the blue filter, displaying varying emission colors.

Figure 7. Fluorescence images of PE, PP, PS, and PET polymers stained with NR.

ACCEPTED

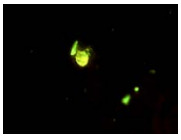
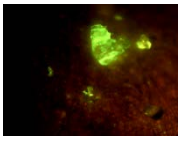
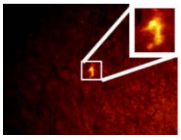
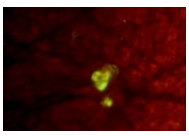
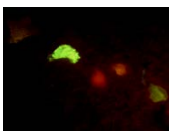
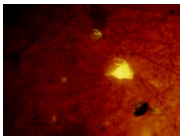
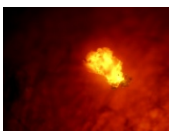
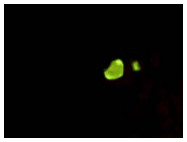
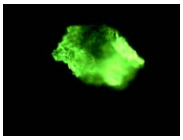
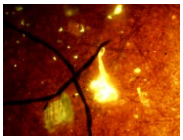
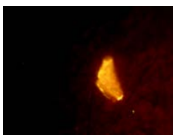


Wilks' Lambda value of 0.660 ($p < 0.001$), indicating significant differences between the groups based on their fluorescence intensities. Groups Centroids revealed that PS (1.023) had the highest centroid value, indicating that it was the most distinct group compared to PP (0.074), PE (-0.204), and PET (-0.775)

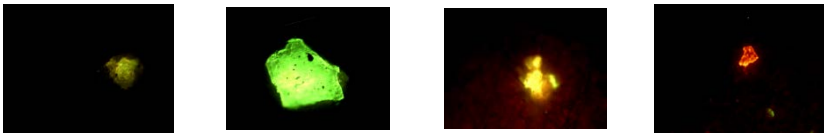
Figure 8. Discriminant Function Analysis (DFA) plot representing group differentiation based on fluorescence intensity, showing partial separation and overlap among PE, PP, PS, and PET.

ACCEPTED

Table 4. Representative Nile Red-positive particles observed in non-fortified commercial feed samples following TMAH-TCM treatment and NR staining. The particles exhibited fluorescence characteristics similar to those of the reference polymers; however, polymer identities were not independently confirmed by spectroscopic analysis.

Feed Materials	MPs			
	PE	**PP**	**PS**	**PET**
Layer Feed				
Calf Starter Feed				
Broiler Feed				

Calf Grower Feed 

Turkey Feed 

ACCEPTED